A STUDY OF DIFFUSION MODELS AND THEIR APPLICATION TO POROUS CATALYSTS

F. Balfanz and D. Gelbin

UDC 678.019.247

A new model of diffusion in porous catalysts is proposed, namely a macropore model. A comparison between test results and calculations indicates a close agreement.

The performance parameters of a reaction with heterogeneous catalysis are largely affected by the processes of heat and mass transfer [1].

The mass transfer in porous materials used as catalysts, because of their large internal surface which participates in the reaction, is determined not only by such parameters as the temperature and the pressure in the liquid but also by the pore structure.

The structure of most porous materials is so complex and irregular, however, that its mathematical description becomes very difficult. It would be of interest, therefore, to consider models which have been proposed during the last decade for the calculation of the effective diffusivity in porous materials [2-5]. An analysis of the results of studies on the subject shows that the purpose of such studies was both to broaden the applicability of these models by appropriate modifications [2-5] and, at the same time, to reveal which model would be most suitable for any particular type of catalyst [6-11].

Latest developments in computer techniques have made it possible to solve problems of diffusion in multicomponent gas mixtures [12-15].

Concerning the experimental studies of diffusion processes in porous materials, it is to be noted that various transient methods of testing have been used more extensively. They have also been compared with steady-state methods, while a few of them have been compared with one another [16-21].

In this study the authors deal essentially with the problem of diffusion models. Inasmuch as the method of analyzing such models has been already described thoroughly in [21, 22] and illustrated on the Satterfield–Cadley model with parallel pores [23], we will list here, without any further explanation, all the equations needed for this analysis:

parallel-pores model [23]

$$D_{\text{eff}} = \frac{D_{pM}}{\tau_p^2} = \frac{1}{\tau_p^2} \sum_{a_{\min}}^{a_{\max}} (1/K_A a + 1/D_N)^{-1} \rho_p \Delta V_g(a); \tag{1}$$

random-pores model [3]

$$D_{\text{eff}} = \varepsilon_a^2 D_a + (1 - \varepsilon_a)^2 D_i + \frac{4\varepsilon_a (1 - \varepsilon_a)}{1/D_a + 1/D_i}; \tag{2}$$

modified random-pores model [19]

$$D_{\text{eff}} = \sum_n \varepsilon_n \sum_j \varepsilon_j D_{nj} + \left[\left(1 - \sum_j \varepsilon_j\right)/2\right]^2 D_{ii} + \left[\sum_n 4\varepsilon_n \left(1 - \sum_j \varepsilon_j\right)/2\right] D_{ni}; \tag{3}$$

Central Institute of Physical Chemistry, German Academy of Sciences, Berlin. Translated from Inzhenerno-Fizicheskii Zhurnal, Vol. 25, No. 4, pp. 708-719, October, 1973. Original article submitted September 26, 1972.

© 1975 Plenum Publishing Corporation, 227 West 17th Street, New York, N.Y. 10011. No part of this publication may be reproduced, stored in a retrieval system, or transmitted, in any form or by any means, electronic, mechanical, photocopying, microfilming, recording or otherwise, without written permission of the publisher. A copy of this article is available from the publisher for $15.00.

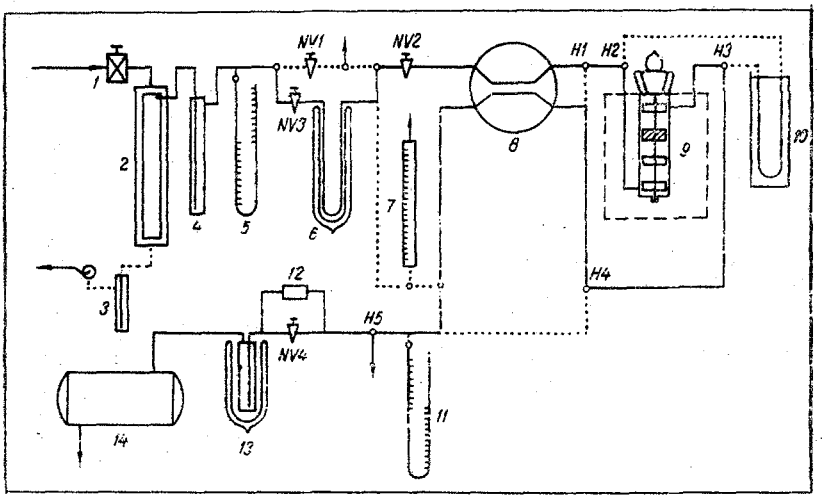

Fig. 1. Schematic diagram of the apparatus for parahydrogen conversion: 1) reductor; 2) hydrogen purification; 3) capillary; 4) instrument for measuring the dynamic pressure head; 5) mercury manometer; 6) converter No. 1; 7) instrument for measuring the soap film; 8) chamber for heat conduction measurement; 9) reactor; 10) converter No. 2; 11) mercury manometer; 12) capillary; 13) cooler trap; 14) vacuum pump; NV) needle valve; H) three-way tap; solid line follows the reaction flow path; dotted line follows the reference path.

efficiency and Tiehle modulus [24]

$$\eta = \frac{k}{k_0} = \frac{1}{h}\left[\frac{1}{\tanh 3h} - \frac{1}{3h}\right]; \tag{4}$$

$$h = \frac{A}{3}\left(\frac{\rho_p S_g k_0}{D_{\text{eff}}}\right)^{1/2}; \tag{5}$$

permeability formula [22]

$$\tau_p^2 = \frac{F\Delta p}{NLRT}\sum_{a_{\min}}^{a_{\max}}\left(K_A a + \frac{a^2\bar{p}}{8\gamma}\right)\rho_p \Delta V_g(a). \tag{6}$$

We will also use the Vakao–Smith equation [3] or the Cunningham–Geankoplis equation [9] for the random-pores models. Only data on the porosity and the size distribution of pores in the catalyst are needed for determining the effective diffusivity on the basis of these models, while exact diffusion and permeability measurements are required for determining the sinuosity factor τ_p in the Satterfield–Cadley parallel-pores model. In this study we have tried to develop a method which would dispense with such measurements. This can be achieved on the premise that the diffusion process and the reaction occur simultaneously, with the distribution of micropores and macropores assumed to be statistical. Such a size distribution will be different in catalyst powder and catalyst pellets, however, and not the same in a compact pellet as in a flimsy pellet.

In such a system, therefore, one must consider two opposing effects associated, during the diffusion process and the reaction, with a changing ratio of macropores to micropores, inasmuch as the diffusion in impeded more in pellets of a higher density, while, on the other hand, the reaction is impeded less in a volume with a larger per unit internal surface.

With this in mind, we proceed as follows. The internal surface formed by micropores, in pellets as well as in a powder bed, will be distributed over corresponding macropore volumes. On such a basis, the equilibrium equation is now

$$D_{p\text{эф}}\left(\frac{\partial^2 c}{\partial a^2} + \frac{2}{a}\frac{\partial c}{\partial a}\right) + \rho_p k_0'' \frac{S_g}{v_a} c = 0. \tag{7}$$

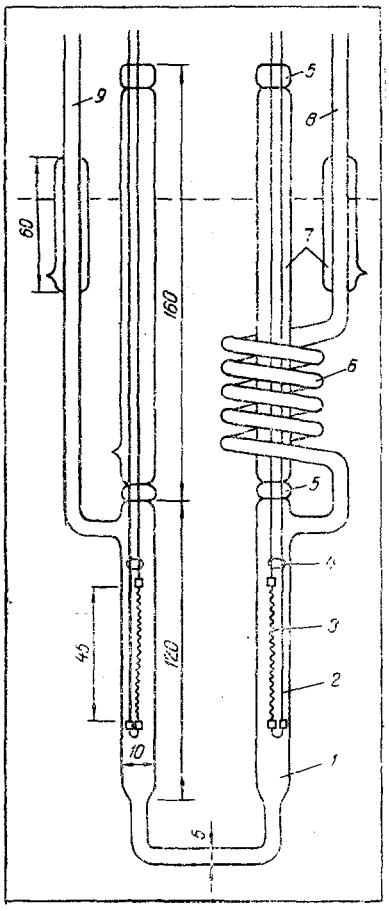

Fig. 2

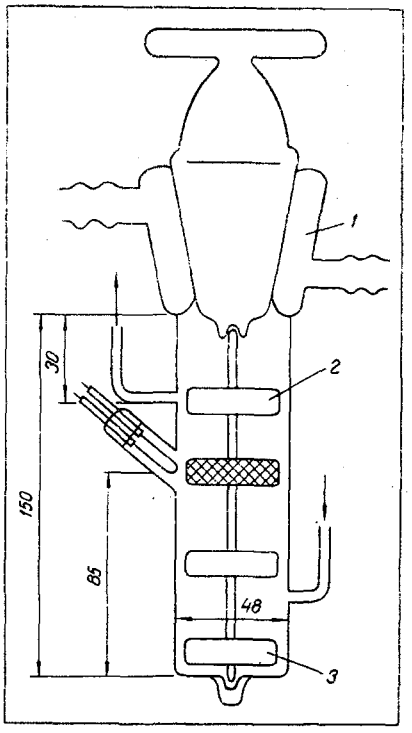

Fig. 3

Fig. 2. Glass-type heat-conduction meter: 1) measuring chamber; 2) tungsten feeder wire; 3) heater wire; 4) glass bead; 5) spacer; 6) cooling coil; 7) evacuated glass tube; 8) gas inlet; 9) outlet.

Fig. 3. Reactor with stirrer: 1) cooling jacket; 2) basket of copper-wire mesh; 3) iron rods.

The diffusivity D_{pm} here is calculated according to Eq. (1) for the parallel-pores model.

Contrary to earlier derivations which have led to Eq. (5), not the "diffusion" term is corrected here by introducing the sinuosity factor and thus the effective diffusivity but, instead, the "source" term. As a result, the reaction rate constant is referred to the free volume of macropores rather than to the catalyst surface. The relation for k_0'' is then

$$k_0'' = k_0' \frac{v_a^0}{S_g^0}. \tag{8}$$

In Eq. (7) V_a denotes the volume of macropores in pellets, while v_a^0 in (8) denotes the volume of macropores in powder. All this applies also to the respective internal surfaces S_g and S_g^0. The volume of macropores in a powder mass v_a^0 is found in the course of conventional porosity measurements by the mercury-porometer method.

According to (7), the Tiehle modulus can be defined as

$$h = \frac{A}{3}\left(\frac{\rho_p k_0' S_g}{D_{pm} v_a}\right)^{1/2}. \tag{9}$$

This expression, in turn, together with (1) and (5) yields for the sinuosity factor

$$\tau_м^2 = \frac{v_a^0 S_g}{v_a S_g^0}. \tag{10}$$

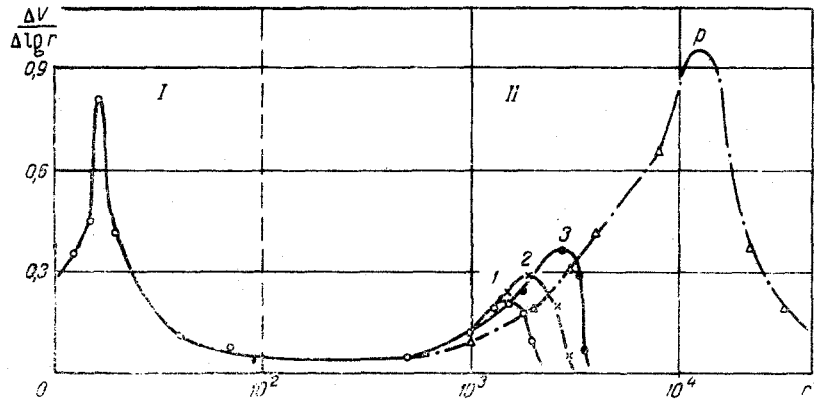

Fig. 4. Size distribution of pores: I) micropore range; II) macropore range; 1, 2, 3) pellets; r, Å.

This expression indicates that any difference in internal surface between powder and pellets is compensated by the corresponding ratio of macropore volumes.

Unlike in the earlier method based on the Satterfield–Cadley model, here the sinuosity factor can be determined from the structural parameters of the catalyst.

Insofar as it is evident now that the lower efficiency of catalyst pellets produced under higher molding pressure is essentially due to a reduced volume of macropores, we are calling the model based on Eqs. (9) and (10) the "macropores" model.

As the control reaction for the study of the diffusion model we used the conversion of parahydrogen. Such a reaction seemed particularly suitable for this purpose, because: 1) the reactant and the product are chemically identical; 2) no side reactions occur; 3) the equation for the reaction rate is simple; 4) the kinetics of this process are simple; and 5) the change in enthalpy at the accommodation temperature is minimal.

Apparatus and Catalyst. For determining the reaction rate constant we used the following apparatus schematically shown in Fig. 1. Normal hydrogen for the measurements was purified in a silver–palladium diaphragm cell and converted to 50% parahydrogen in converter No. 1. The nickel oxide catalyst for the conversion process was immersed in this converter and cooled down to –196°C with liquid nitrogen. The parahydrogen was completely inverted to standard gas in converter No. 2, for the determination of the volume reaction in the reactor. Here we used platinum as the catalyst. The pressure was set to various levels by means of a needle valve.

The hydrogen mixture was analyzed with a heat-conduction meter (Fig. 2) which had been specially designed and installed for this purpose, because other available gas analyzers were not sensitive enough.

The heater wire was a spiral filament from an incandescent lamp, with a resistance of 35 Ω. This filament and the leads were made of tungsten.

In order to reduce the fluctuations in pressure and drag which could occur during measurements of the liquid level in the cooling tank, the top parts of the instrument were either evacuated or protected with a glass "jacket" which had also been evacuated.

For the reactor we used a catalytic reactor with a stirrer (Fig. 3) similar in construction to the reactor described in [25, 26]. Its capacity was 225 cm^3. The catalyst was placed in a basket made of a copper-wire mesh. For replacing the test specimens, the stirrer shaft could be taken out of the reactor and its upper two blades could be removed. The reactor was placed in an air thermostat, the latter heated with various incandescent lamps.

The temperature was measured with a copper–constantan thermocouple which, without a protective sheath, had been mounted at the catalyst level. The maximum fluctuation did not exceed ±0.2°C throughout the test.

The catalyst for the conversion of parahydrogen was a mixture of aluminum–silicon oxide and nickel oxide, as the active component, with an admixture of 2.5% graphite as binder. The structural characteristics of the catalyst powder were: internal surface 225 ± 10 m^2/g, volume of micropores 0.400 ± 0.020 cm^3/g, volume of macropores in the loose powder bed 0.710 ± 0.020 cm^3/g, true density 2.52 ± 0.06 g/cm^3,

TABLE 1. Structural Characteristics of Catalyst Pellets

Characteristics	Grade of pellets		
	1	2	3
Molding pressure, tons/cm^2	1.72	2.45	3.18
Diameter, cm	0.495	0.49	0.49
Density, g/cm^3	1.086	1.194	1.255
Internal surface, m^2/g	225	225	225
Volume of macropores, cm^3/g	0.184	0.136	0.104
Volume of micropores, cm^3/g	0.400	0.400	0.364
Macroporosity	0.200	0.162	0.131
Microporosity	0.435	0.478	0.457
Most frequent radius of macropores, Å	2800	1900	1500

TABLE 2. Reaction Rate Constant Determined Experimentally, 10^6 cm/sec

Pressure, torr	Temperature, °K	Powder		Grade 1		Grade 2		Grade 3	
		k_0	±%	k_0	±%	k_0	±%	k_0	±%
760	393.2	16.60	7.1	5.65	3.0	3.90	7.2	2.76	10.3
	378.6	12.90	6.5	4.68	3.0	3.21	8.0	2.27	9.7
	364.5	9.40	8.3	3.92	4.5	2.58	9.2	1.81	9.7
	348.6	6.45	8.1	3.02	5.5	1.99	10.6	1.39	9.6
	333.5	4.55	8.0	2.43	10.1	1.52	12.8	1.09	8.8
355	378.6	15.90	6.7	6.66	4.0	3.98	6.4	3.11	12.5
	364.5	11.60	7.7	5.28	5.0	3.18	5.1	2.46	13.2
	348.6	8.25	8.9	4.21	6.5	2.63	6.2	1.91	11.9
	333.5	5.45	9.0	3.30	10.0	1.91	5.6	1.45	12.1
120	364.5	16.35	5.2	7.90	5.0	4.45	8.5	3.32	13.3
	348.6	11.80	7.7	6.19	6.5	3.45	10.4	2.65	12.2
	333.5	7.65	9.8	4.92	10.2	2.61	10.3	2.02	13.2

the most frequent radius of micropores 16.5 Å, the most frequent radius of macropores 13,000 Å; the structural characteristics of catalyst pellets were as listed in Table 1.

The size distributions of pores have been plotted in Fig. 4 from measurements by the BET method, and from porometric tests for macropores in the size range from 100 Å up. In Fig. 4 is also shown the size distribution of macropores in a loose powder bed of particles smaller than 80 μ. The curves here indicate clearly how the peaks decrease as the molding pressure is raised, i.e., how the volume of macropores and their effective radius decrease under higher molding pressure.

Kinetic Measurements. In the apparatus for the conversion of parahydrogen we determined the conversion level, as a function of the temperature and the pressure as well as of the permeability and the pellet density. The temperature was varied from 60 to 120°C and the consumption rate was varied from 3.7 to 18.5 liters/h. The measurements were made at three pressure levels: 760, 350, and 120 torr. The density of the three grades of pellets was 1.086, 1.195, and 1.255 g/cm^3, respectively. Powders were measured with particles smaller than 100 μ and smaller than 80 μ.

The process rate constant was determined graphically from the initial reaction rate, by the method of power series. For this purpose, the logarithm of the reaction rate was plotted versus the logarithm of the unconverted remainder mass. The slope of the resulting straight line determined then the order of the reaction, which in this case was equal to unity.

The experiment has revealed that the laminar boundary layer has no significant effect on the results of kinetic measurements; owing to the high rate of hydrogen diffusion, a stirrer becomes practically unnecessary here.

The test values of the reaction rate constant are shown in Table 2. The apparent activation energy in the process was calculated from the kinetic measurements and found to be, on the average, 3.9 kcal/mole for catalyst pellets and 5.8 kcal/mole for catalyst powder.

The values of the sinuosity factor shown in Table 3 were calculated on the basis of the Satterfield–Cadley parallel-pores model (τ_p) and also on the basis of our proposed "macropores" model (τ_m). For the calculation of τ_p according to Eq. (6) we performed appropriate permeability measurements on three

TABLE 3. Sinuosity Factor Based on the Macropores Model and on Permeability Measurements

Grade	v_g^0	r_0	S_g^0	S_g	τ_M	τ_p	Difference, %
			Conversion of parahydrogen				
Powder	0,709		225		1,00		
1		0,184		225	1,96	1,87	4.6
2		0,136		225	2,28	2,00	12.3
3		0,103		205	2,50	2,03	18,8
			Decomposition of cumene				
Powder	0,672		280		1,00		
1		0.302		280	1,49		
2		0,253		280	1,63	1.80	10.4
3		0,184		280	1.91	1.95	2.1
4, 7, 8		0,081		250	2,73	2,80	2,8
5		0,033		175	3,56	3,10	12,9

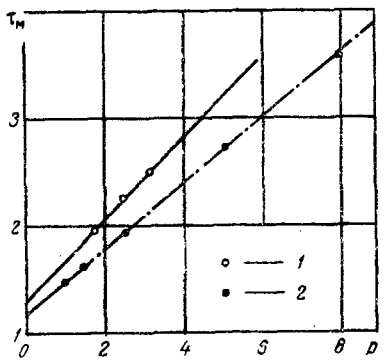

Fig. 5

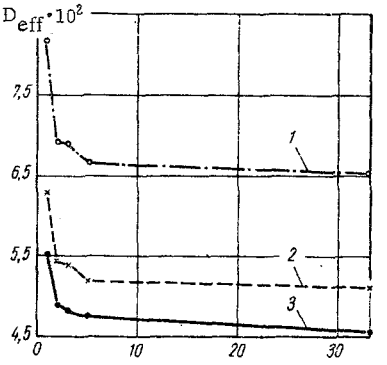

Fig. 6

Fig. 5. Sinuosity factor τ_m as a function of the molding pressure p. 1) Conversion of parahydrogen; 2) decomposition of cumene.

Fig. 6. Diffusivity D_{eff} (10^2 cm^2/sec) as a function of the macropores range (grade 1 pellets): 1) T = 60.3°C and p = 120 torr; 2) 60.3 and 120 [sic]; 3) 120.0 and 355.

grades of catalyst pellets. The resulting values of the sinuosity factor were 1.87, 2.00, and 2.03, respectively – in complete agreement with the test results obtained by Grachev [20], Kirillov [21], and Satterfield–Cadley [23].

For the calculations of τ_m according to Eq. (10) we used data on the catalyst structure. The discrepancy between τ_p and τ_m values was found to be within 4.6-18.8%.

In order to establish the feasibility of using the "macropores" model for evaluating other reactions as well, we analyzed the results which Just had obtained in his study of cumene decomposition [27]. The data shown in the lower part of Table 3 indicate a close agreement between τ_p and τ_m values for this process.

The sinuosity factor τ_m in pellets, as a function of the molding pressure, is shown in Fig. 5 for both reactions. The linearity of this relation makes it feasible to set up an equation for calculating the sinuosity factor. In order to this, however, it is still necessary to study various other types of catalysts.

Knowing the sinuosity factor of pores, one can calculate the effective diffusivity according to the Satterfield–Cadley model (Eq. (1)) and then, on the basis of the obtained values, evaluate the results of measurements pertaining to the kinetic parameters of a reaction. According to the Vakao–Smith model or the Cunningham–Geankoplis model, the diffusivity depends on the number of size ranges into which the macropores are subclassified.

In this study we also considered the effect which such a subdivision of the macropores size spectrum will have on the resulting values of diffusivity. For this purpose, the macropores size spectrum was subdivided successively into two, three, five, and more ranges.

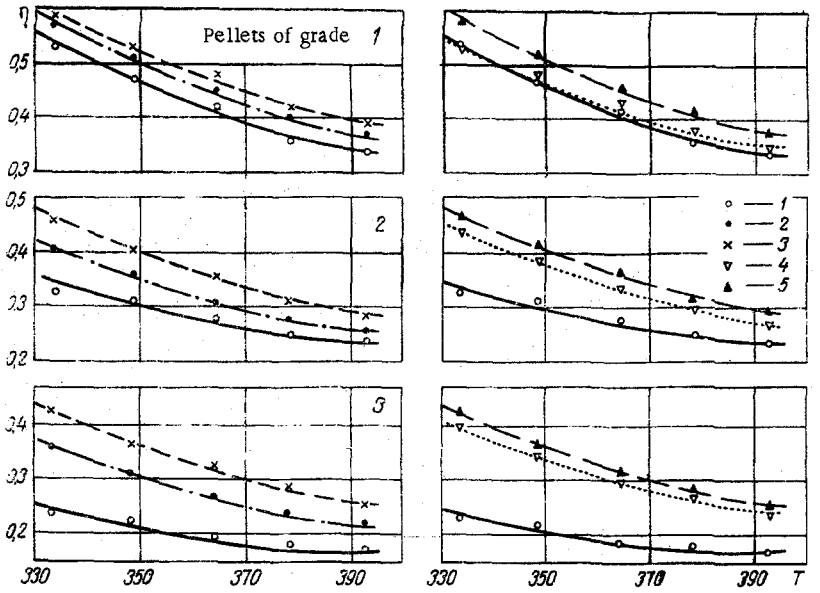

Fig. 7. Efficiency η as a function of the temperature T (°K), under normal pressure (parahydrogen conversion): 1) test; 2) "macropores" model; 3) Satterfield–Cadley model; 4) Cunningham–Geankoplis model; 5) Vakao–Smith model.

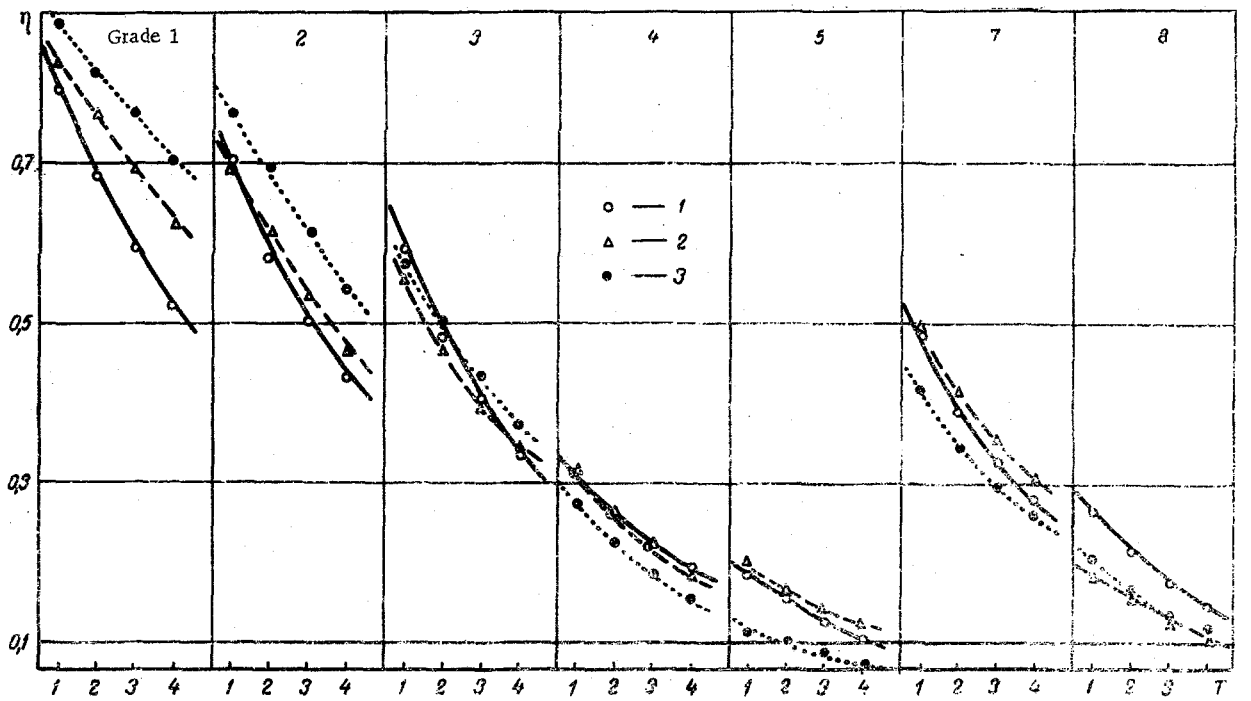

Fig. 8. Efficiency η as a function of the temperature T (cumene decomposition): 1) test data; 2) Vakao–Smith model; 3) "macropores" model.

The results are shown in Fig. 6. Already a subdivision into two ranges makes a large difference, as compared with the original value, but further subdivisions make only small further differences.

Comparison between Tested Values and Theoretical Values of Efficiency. The theoretical efficiency was determined on the basis of the Vakao–Smith model, the Cunningham–Geankoplis model, and the Satterfield–Cadley model.

The temperature characteristics of efficiency, both measured and calculated according to the three diffusion models, are shown in Fig. 7. It is quite evident here that the Vakao–Smith model [3] yields a fair agreement with test data.

As to the Cunningham–Geankoplis model [19], it should be used only when the pores size spectrum is wide; otherwise, the unwieldy calculations here lose their validity.

The efficiency of the cumene decomposition reaction, based on test as well as calculated according to the "macropores" model and the Vakao–Smith model, is shown in Fig. 8. Both models yield a close agreement with test values. The differences between test values and those based on the "macropores" model are within 6.3-20.2%.

The comparison between values based on the Satterfield–Cadley model and on the "macropores" model, respectively, indicates that the latter model developed by us yields a much closer agreement with tests. It must be considered, moreover, that this model minimizes testing time and labor: it makes permeability and diffusion measurements unnecessary.

NOTATION

a	is the pore radius, cm;
A	is the particle radius, cm;
c	is the molar concentration, mole/cm^3;
D_{eff}	is the effective diffusivity, cm^2/sec;
D_{index}	is the diffusivity referred to the macropores range (a, n, j), to the micropores range (i, ii), or to the transition range (ni), respectively, cm^2/sec;
D_N	is the normal diffusivity, cm^2/sec;
D_{pm}	is the diffusivity according to the parallel-pores model, cm^2/sec;
F	is the cross-section area, cm^2;
h	is the Tiehle modulus, cm^2;
k	is the rate constant of a first-order reaction at catalyst pellets, cm/sec;
k_0	is the rate constant of a first-order reaction, the diffusion effect disregarded, cm/sec;
k_0'	is the reaction rate constant, cm^3/g·sec;
k_0''	is the reaction rate constant defined according to Eq. (8), cm^3/g·sec;
$K_A = 9.7 \cdot 10^3 (T/M)^{1/2}$, cm/sec;	
L	is the particle length, cm;
M	is the molecular weight;
N	is the transport rate, cm^3/sec;
Δp	is the pressure difference (p_1, p_2), torr;
$\bar{p}$	is the mean pressure, torr;
p_1, p_2	are the penetration pressures, before and behind pellets, respectively, torr;
R	is the gas constant, torr·cm^3;
S_g	is the internal surface of catalyst pellets, cm^2/g;
S_g^0	is the internal surface of catalyst powder, cm^2/g;
T	is the absolute temperature, °K;
v_a	is the volume of macropores in catalyst pellets, cm^3/g;
v_a^0	is the volume of macropores in catalyst powder, cm^3/g;
$V_g(a)$	is the volume of pores with any one radius a, cm^3/g;
ε	is the porosity;
ν	is the dynamic viscosity, torr·sec;
ρ_p	is the pellet density, g/cm^3;
τ_p	is the sinuosity factor according to the parallel-pores model;
τ_m	is the sinuosity factor according to the "macropores" model.

LITERATURE CITED

1. G. Emig, Fortschritt Chem. Forschung, 13, 451 (1970).
2. C. N. Satterfield, Mass Transfer in Heterogeneous Catalysis, MIT Press, Cambridge Mass. (1970).
3. N. Vakao and J. M. Smith, Chem. Engrg. Sci., 17, 825 (1962).
4. D. Nicholson and J. H. Petropoulos, Brit. J. Appl. Phys., 1, 1379 (1968).
5. R. N. Foster and J. B. Butt, AIChEJ, 12, 180 (1960).
6. G. R. Youngquist, Industr. Engrg. Chem., 62, 52 (1970).
7. J. S. Sterrey and L. F. Brown, AIChEJ, 14, 696 (1968).

8. L. F. Brown, H. W. Haynes, and W. H. Manogue, J. Catalysis, 14, 220 (1969).
9. R. S. Cunningham and C. J. Geankoplis, IEC Fundamentals, 7, 535 (1968).
10. M. R. Rao, N. Vakao, and J. M. Smith, IEC Fundamentals, 3, 127 (1964).
11. D. Gelbin and H. J. Just, Chem. Technik, 23, 581 (1971).
12. Ya. A. Sokolinskii and N. A. Krasnoborov, Teor. Osnovy Khim. Tekhnolog., III, 551 (1969).
13. R. R. Reshetov, Zh. Fiz. Khim., 44, No. 12, 3057 (1970).
14. R. R. Remick and C. J. Geankoplis, IEC Fundamentals, 9, 206 (1970).
15. R. S. Cunningham and C. J. Geankoplis, IEC Fundamentals, 9, 429 (1968).
16. G. A. Grachev, K. G. Ione, and A. A. Barshev, Kinetika i Kataliz, 11, No. 2, 541 (1970).
17. R. L. Cerro and J. M. Smith, AIChEJ, 16, 1034 (1970).
18. G. A. Grachev and K. G. Ione, Kinetika i Kataliz, 11, No. 3, 765 (1970).
19. G. A. Grachev, K. G. Ione, and A. A. Barshev, Kinetika i Kataliz, 11, No. 4, 1041 (1970).
20. G. A. Grachev, V. S. Beskov, K. G. Ione, O. A. Malinovskaya, and M. G. Slin'ko, Kinetika i Kataliz, 12, No. 5 (1971).
21. V. A. Kirillov, Yu. Sh. Matros, V. A. Kuzin, and M. G. Slin'ko, Kinetika i Kataliz, 12, No. 1, 219 (1971).
22. H. J. Just and D. Gelbin, Chem. Technik, 23, 648 (1971).
23. C. N. Satterfield and P. J. Cadley, Industr. Engrg. Chem., Process Design Development, 7, 256 (1968).
24. A. Wheeler, Advanc. Catalysis, 2 (1951).
25. J. J. Carberry, Industr. Engrg. Chem., 56, 33 (1964).
26. M. L. Brisk, R. L. Day, M. Jones, and J. B. Warren, Trans. Inst. Chem. Engr., 46, No. 3 (1968).
27. H. J. Just, Dissertation, Berlin (1971).